Frontiers in Scientific Research and Technology

Online ISSN: 2682-2970
Print ISSN: 2682-2962
http://fsrt.journals.ekb.eg

FSRT J 9 (2024) 100 - 116 10.21608/fsrt.2024.302366.1131

Variations in Calcareous Nannofossil Assemblages and paleoenvironmental studies on the Danian – Selandian Succession at the Qreiya area, East Qena, Eastern Desert, Egypt

Mahmoud Faris[1], Ramadan M. El-Kahawy[2], and Atef M. Kasem[3*]

[1] Geology Department, Faculty of Science, Tanta University, Tanta 31527, Egypt.

[2] Geology Department, Faculty of Science, Cairo University, Giza 12613, Egypt.

[3] Geology Department, Faculty of Science, Damanhour University, Damanhour 22511, Egypt.

ARTICLE INFO

Article history:
Received 9 July 2024
Received in revised form 8 August 2024
Accepted 9 August 2024
Available online 19 August 2024

Keywords
Calcareous nannofossils,
Danian,
Qreiya,
Late Danian Event (LDE),
Egypt.

ABSTRACT

Calcareous nannofossil biostratigrapgic and paleoenevironmental studies were carried out on a 20 m of the Paleocene Dakhla Formation at the Qreiya section (East Qena, Eastern Desert, Egypt). The Late Danian Event (LDE) bed was included in this study. Four zones (CNP4, CNP5, CNP6 and CNP7) and two subzones (CNP5a and CNP5b) were delineated according to the zonal scheme of Agnini et al. (2014). Several species were suggested as new ones that belong to genera *Diantholitha*, *Lithoptychius*, *Pontosphaera* and *Lapideacassis*. The biostratigraphic significances of *Chiasmolithus edentulus*, *Sphenolithus primus, Diantholitha* sp. *Lithoptychius* sp., *Prinsius* spp., *Braarudosphaera bigelowii* as well as radiative episodes of fasciculiths were discussed in this research. The Danian-Selandian boundary is tentatively traced within Zone CNP7. Calcareous nannofossil data suggest mesotrophic and cool-water conditions during most of the study interval. However, warm-water conditions prevailed the lower part of this interval as well as the basal part of the LDE interval.

1. Introduction

The Paleocene time interval was characterized by biotic and environmental changes. Short-term and highly warm events resulted in lithological, chemical and biotic changes during this interval (Schmitz et al., 2011). Among these episodes are the Latest Danian Event (LDE) in addition to the Danian /Selandian (D/S) transition event (Quillévéré et al., 2002, 2008; Speijer, 2003b; Schmitz et al., 2011; for more references see Kasem et al., 2022 and Kasem, 2023). These hyperthermals were globally associated with geochemical and biotic changes (Schmitz et al., 2011 and Kasem, 2023 for more references)

The Qreiya section is a complete Danian-Selandian section in the Tethyan region (Schmitz et al., 2011). Several authors investigated it for stratigraphic and calcareous nannofossil taxonomic purposes. Among them are Knox et al. (2003); Rodriguez and Aubry (2006); Sprong et al. (2009), and Monechi et al. (2013). Significant variations in the Paleocene calcareous nannofossils took place in Zone NP4 (Aubry, 1998; Bernaola et al., 2009; Schmitz et al., 2011). This study is aiming to track the biotic and paleoecological variations across the Danian-Selandian succession at Qreiya area in terms of calcareous nannofossil assemblages.

* Corresponding author at Damanhour University

E-mail addresses: kasematef@sci.dmu.edu.eg (Atef M. Kasem)

Fig. 1: Location map for the area of the study section.

2. Geologic setting

The epicontinental shelf of southern Tethys encompassed Egypt in the past. During Early Paleogene, the essential structural units controlled the sedimentation in

Egypt from south to north were the Arabian–Nubian massive, “Stable Shelf”, and “Unstable Shelf”, respectively (Said, 1962). The Paleocene Tethys Sea highly transgressed and thus the large part of southern Egypt was flooded (Fig. 2). Barazi and Kuss (1987) reported that this transgression of the Tethys Sea reached northern Sudan. The Egyptian shelf acted as a carbonate platform and siliciclastic system, thus carbonates and shales accumulated (Aubry and Salem, 2013b). As such, the Paleocene interval in Egyptian sections records in detail the biologic and chemical changes across this interval. Paleocene successions in Egypt had subjected to several paleontological and paleoecological studies (see Kasem et. al., 2017 and 2022).

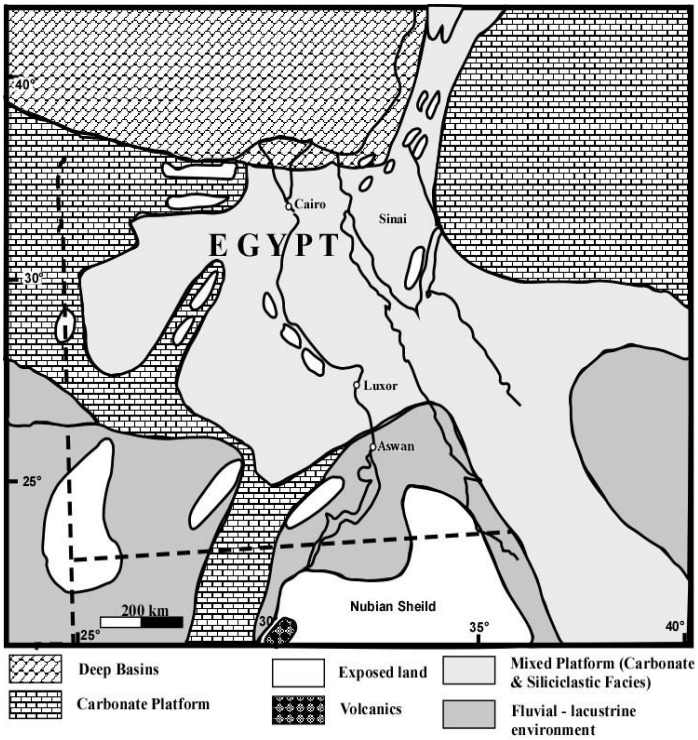

Fig. 2: shows a Paleocene paleogeographic map of the Africa- Arabian region (modified after Guiraud and Bosworth, 1999).

3. Materials, methods and depository

Seventy-one samples were investigated from the Paleocene at Qreiya area, which is located at latitudes 26° 21' N and longitudes 33° 01' E, about 50 km ENE of Qena town in upper Egypt (Fig. 1). This section is referred to by several authors as Qreiya 1 (see Aubry et al., 2012 for references). The lithostratigraphy as well as calcareous nannofossils marker species of the study interval are shown in Figure 3.

For calcareous nannofossil examination, pipette strew slides were prepared for each sample (see Kasem and Kassab, 2023). An Euromex Iscope light microscope were utilized at magnification of 1250X. The counts of the species defined in this research are presented in Table 1. Microscopic photographs of selected taxa are shown on plates 1-3.

The quantitative datasets of the retrieved calcareous nannofossil taxa were processed for multivariate statistical analysis. For only the taxa higher than 0.3% of the total percentage, the non-metric multidimensional scaling (nMDS) has been performed. The nMDS analysis was accomplished via 2D dimensionality type and Bray- Curtis as a similarity index, with emphasis on the first two nMDS axes. The analysis was applied based on two modes (R; species, and Q; sample) using PAST 4.13 software (Hammer et al., 2001). The materials used for this study are deposited at Tanta University, Faculty of Science, Geology Department, Tanta, Egypt.

4. Lithostratigraphy

The samples investigated in this research belong to the Dakhla Formation, which had been first introduced by Said (1961). It is composed of a shale succession at its type locality at the Dakhla Oasis (long scarp north of Mut). It overlies the Duwi Phosphate and is overlain by the Tarawan Formation. At this type locality, this unit is about 130 m of shales, marls, and clays intercalated with calcareous sandy and silty beds (Awad and Ghobrial, 1965). The study interval is spanning Danian-Selandian Age (Aubry et al., 2012). The lower part of this formation north of latitudes 26° 30' in Egypt is generally laterally equivalent to the carbonate facies of the Sudr Formation or its lateral equivalent, the Khoman Formation (Faris and Farouk, 2012).

Awad and Ghobrial (1965) documented that the Dakhla Shale at Kharga Oasis had been divided into three members (Mawhoob Shale, Beris Oyster Mudstone, and Kharga Shale members, respectively from base to top). The interval lies between the middle and upper members were assigned to the "Teneida Member" in the area northwest of Kharga Oasis (Omara et al. 1976). A further subdivision of this formation had been suggested by Abdel Razik (1972). He differentiated the older Hamama Marl Member from the younger Beida Shale Member. Furthermore, a distinct marker bed (~ 25 cm thick) was recorded in several Egyptian sections in the upper interval of this formation. This bed had different names. Among them are the D/S transition, “Neo-Duwi”-event, ‘El-Qreiya Bed, Late Danian Event (LDE) and the Neo-Duwi beds (Speijer, 2003a, b; Guasti et al., 2005; Soliman and Obaidalla, 2010; Sprong et al. 2011, and Aubry et al., 2012). This marker bed was assigned to Selandian (Speijer, 2003a, b; Guasti et al., 2005; Bornemann et al., 2009; Obaidalla et al., 2009, and Youssef, 2009). Later, it was revealed that this bed occurs in the Danian interval (Sprong et al., 2009, 2011). The Qreiya beds at Qreiya 1 section was differentiated by Soliman and Obaidalla (2010) into four bands. Aubry et al. (2012) subdivided the 20 meter thick Qreiya 1 section into seven lithological units. They recognized three distinct lithological markers (unit 2, Neo-Duwi beds A-D, and unit 6, Fig. 2). They documented that units 1, 3, 5, and 7 are 4 m, 9 cm, 87 cm and 5.6 m thick of olive-grey mudstone, respectively (Aubry et al., 2012). Furthermore, unit 2 is the lowest marker bed and consists of 11 cm of homogenous pale-grey siltstone and its base represents the level 0 of the measured section

(Aubry et al., 2012). Moreover, unit 4 is 8.97 m thick of dark grey claystone. Unit 6 is the highest marker bed and consists of 5 cm thick, brown, organic rich shale with plant fragments (Aubry et al., 2012). Neo-Duwi beds (A, B, C, and D) are the middle phosphate bearing marker and consist of 31 cm of fissile mudstone with coprolites. Aubry et al. (2012) described these bands as follows: Bed A: 5 cm of black laminated mudstone with rare coprolites; Bed B: 7 cm of organic-rich brown grey shale, friable and moderately laminated, with abundant plant fragments and phosphatic material; Bed C: 10 cm of indurated, grey shale with scattered coprolites, and Bed D: 8 cm of organic-rich brown grey shale with coprolites and plant fragments, moderately laminated.

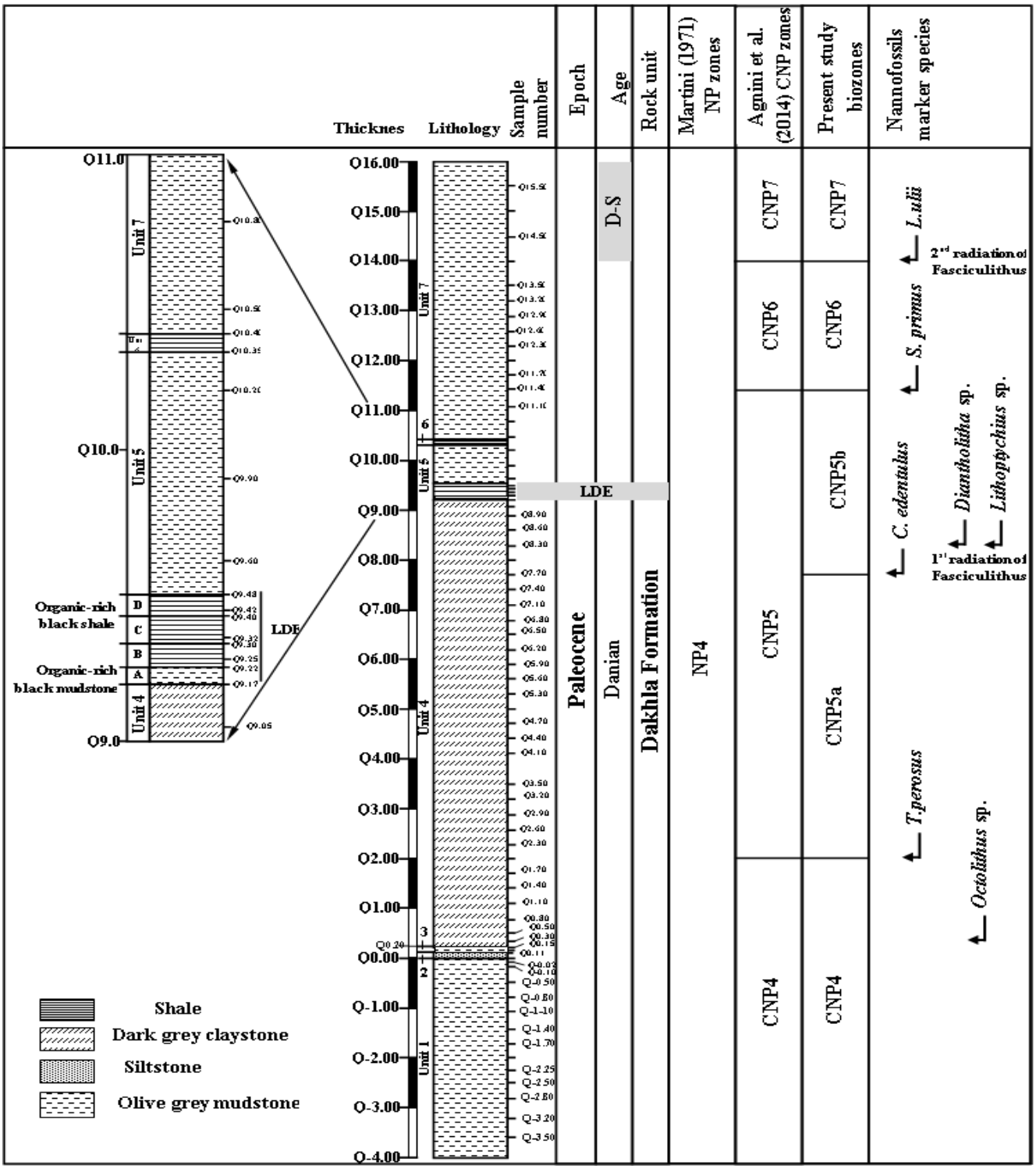

Fig. 3: shows lithology of the Qreiya section (re-drawn after Aubry et al., 2012).

5. Biostratigraphy

The 20 m thick interval of this study belongs to Zone NP4 of Martini (1971). It covers from the lowest occurrences (LOs) of *Ellipsolithus macellus* and *Fasciculithus tympaniformis*. Varol (1989) documented that this interval covers Subzone NTp5c, plus Zones NTp6-8. He also subdivided Zone NTp7 into two subzones and Zone NTp8 into three subzones. He delineated the limits of these biozones based on the HOs of *Neocrepidolithus cruciatus, Neochiastozygus eosaepes*, and/or *N. imbriei*, the LO of *Chiasmolithus edentulus*, the LO of *Sphenolithus primus*, and/or *Lithoptychius chowii*, the LOs of *L. ulii* and *L. billii*, the LOs of *L. pileatus*, *L. janii*, *F. involutus*, and *F. tympaniformis*, respectively. Quillévéré et al. (2002) differentiated Subzone NP4a from Subzone NP4b by the LO of *S. primus*. Agnini et al. (2014) delineate the base of Zones CNP4, CNP5, CNP6, and CNP7 by the LOs of *Toweius pertusus*, *Chiasmolithus edentulus*, *S*. *primus*, and *Lithoptychius ulii*, respectively. This zonation was followed in this work, however, the *S*. *primus*'s lowest continuous occurrence (LCtO) was adopted instead of its LO (Fig. 2, and Table 1). Five calcareous nannofossil biozones were recognized as follows.

a. *Prinsius martinii* Zone (CNP4); it covers between the LOs of *Prinsius martinii* and *Toweius pertusus* respectively. It spans the lower 6 m of the study interval (Fig. 3).

b. *Toweius pertusus* Zone (CNP5); it covers between the LO and LCtO of *Toweius pertusus* and *Sphenolithus primus*, respectively. This interval spans ~ 9.40 m at Qreiya (Fig. 3). It is further subdivided into:

i. Subzone CNP5a; it covers between the LOs of *Toweius pertusus* and *Chiasmolithus edentulus*, respectively. It spans ~ 5.70 m at Qreiya (Fig. 3).

ii. *Chiasmolithus edentulus* Subzone (CNP5b); it covers between the LO and the LCtO of *Chiasmolithus edentulus* and *Sphenolithus primus*, respectively. It correlates Varoli' (1989) Subzone NTp7b. It spans ~ 3.70 m at Qreiya (Fig. 3).

c. *Sphenolithus primus* Zone (CNP6): it spans between the LCtO and LO of *Sphenolithus primus* and *Lithoptychius ulii*, respectively. It correlates Varoli' (1989) Subzone NTp8a. It spans ~ 2.60 m at Qreiya (Fig. 3).

d. *Lithoptychius ulii* Zone (CNP7); it covers between the LOs of *Lithoptychius ulii* and *Fasciculithus tympaniformis*. It correlates the Varoli' (1989) Subzones NTp8b-c. It spans the uppermost 2 m of the study interval (Fig. 3). Varol (1989) depended on the entries of *L. pileatus, L. janii,* and/or *L. involutus* to subdivide the interval equivalent to this zone into subzones NTp8b and NTp8c. In this study, *L. ulii* and *L. billii* first appeared together, and are followed by the co-occurrences of *L. janii*, and *L. pileatus* (Table 1).

Table 1: Calcareous nannofossil abundances at Danian - Selandian at Qreiya, east Qena, Eastern Desert, Egypt

Epoch	Age	Rock Unite	Martini (1971) NP Zones	Agnini et al. (2014)	NP biozones	QE Sample thickness	Abundance	diversity	*Coccolithus pelagicus*	*Ericsonia robusta*	*Ericsonia subpertusa*	*Thoracosphaera operculata*	*Thoracosphaera heimii*	*Thoracosphaera saxea*	*Zeugrhabdotus sigmoides*	*Cruciplacolithus primus*	*Cruciplacolithus intermedius*	*Cruciplacolithus tenuis*	*Neochiastozygus sp.*	*Prinsius sp.*	*Ellipsolithus macellus*	*Neochiastozygus perfectus*	*Neochiastozygus eeosaepes*	*Chiasmolithus danicus*	*Octolithus sp.*	*Lapideacassis sp.*	*Toweius pertusus*	*Pontosphaera sp.*	*Unknown species*	*Chiasmolithus edentulus*	*Ellipsolithus distichus*	*Diantholitha mariposa*	*Sphenolithus primus*	*Diantholitha alata*	*Diantholitha magnolia*	*Lithoptychius collaris*	*Lithoptychius felis*	*Lithoptychius schmitzii*	*Pontosphaera distincta*	*Lithoptychius varolii*	*Diantholitha sp1.*	*Diantholitha sp2.*	*Lithoptychius sp1.*	*Lithoptychius stenehengi*	*Diantholitha sp3.*	*Lithoptychius sp5.*	*Lithoptychius sp2.*	*Lithoptychius sp3.*	*Lithoptychius sp6.*	*Chiasmolithus consuetus*	*Lithoptychius vertebratoides*	*Lithoptychius chowii*	*Chiasmolithus bidens*	*Lithoptychius sp4.*	*Diantholitha sp4.*	*Cruciplacolithus frequens*	*Fasciculithus involutus*	*Lithoptychius ulii*	*Lithoptychius billii*	*Lithoptychius janii*	*Lithoptychius pileatus*
Paleocene	Selandian	Dakhla Formation	NP4	CNP7	CNP7	QE 16.00	532	20	C	F	A	C	F		C			C		A	F	A		R	R		C		R	C			C											F													F	R		R
						QE 15.50	477	24	F	C	A	C	F		C		R	C		A		A		F	F	R	C			C			C				R							C							R	R						F	R	R	R
						QE 15.00	418	28	C	C	A	C	F		C		C	C		A		A			R		F		R	F			C				R	R						F				R		R	R	R	R	R				F	R	R	R
						QE 14.50	402	25	C	F	A	C	C		C		C	C		A	F	A		C	C		F			C			A	R			F							F		R			R		R	R						F	R		
						QE 14.00	372	25	C	F	A	C	C		C		R	C		A	F	A		R	R		C						C				R	R		R				R		R			R			R		R				R	R		
				CNP6	CNP6	QE 13.50	454	16	C	R	A	C	R		C			C		A	F	A		R	C		F			F			F					R																							
						QE 13.20	369	16	C	C	A	C	C		C		F	C		A	F	A		R	C		C			C			C																												
						QE 12.90	461	15	F	F	A		C	R	C		F	C		A	C	A			F					F			C				R																								
						QE 12.60	442	18	C	F	A	C	F		C			C		A	C	A		F	C		C	F		F			F		R															R											
						QE 12.30	357	16	F	F	A	C	F		C	R	C	C		A	C	A		C	F		F				R	R	R					R																							
						QE 12.00	435	19	C	R	A	C	F		C	R	F	C		A	C	A	F	C	C		C	R	R	C																						F										
						QE 11.70	332	19	F	R	C	C	R		C	F	F	C		A	C	A		R			F			C			R					R						R								F										
	Danian					QE 11.40	642	32	C	R	A	C		R	C		R	C		A	C	A		4	R		C			4		R	R			R	F	R		R			R	R		R	R	R	R		R	R		R		R	R					
				CNP5	CNP5b	QE 11.10	687	32	C	C	A	C	F	R	C	R	F	C		VA	C	A		C	R		C	R		C				R	R	R	R	R		R						R	R		R		R	R		R		R	R					
						QE 10.80	503	27	C	C	A	C	R		R	R	R	C		A	C	A	R	F			F	R		C		R		R	R	R							R		R	R			R	R	R					R						
						QE 10.50	370	21	F	F	A	C	R	R	C		F	C		A	C	A		R				R	R	R		R				R		R												C	F											
						QE 10.30	149	27	F	C	A				F			F	R	F	F	C		F				R		F		R		R	R	R	F	F		R		R		R		R	R	R			F	R		R								
						QE 10.20	164	27	C	C	A	F	R		C			R		C		C		F				R		F		R		F	R	R	R	R						R	R	R	R			R	R	R		R	R							
						QE 9.90	502	26	C	C	A	C	R		C		F	C		A	F	C		R				R		F		R		R	R		R	R		R	R					R	R	R		4					R							
						QE 9.60	1266	29	C	C	A	C	R		C			F		VA	F	C		C				R		R	R	R		R	R	R	R	R		R						R	R	R	R	R	R	R	R									
						QE 9.42	982	21	C	C	A	C	R		R	R		C		VA		R		F						R						R	R	R		R				R		R	R	R	R	R				R								
						QE 9.25	79	18	R	C	C	R			R		R			C		R		R					R				R	R	R	R	R	R		R						R	R															
						QE 9.22	422	5	F	C	C	R					R	R		A		R		R																																					
						QE 9.17	2	2		R	R																																																		
						QE 9.05	164	23	F	C	C	C			C	R		F		A	F	C		R		R		R	R	R	R	R		R	R			R	R	R	R																					
						QE 8.90	40	11	R	F	C	R			F		R			C		F										R		R	R																										
						QE 8.60	302	20	C	C	A	C		R	C			F		A	R	C		R				F						R	R	R	R	R		R	R	R																			
						QE 8.30	389	30	C	C	A	C	C		C	F	F	F		A	F	C		R		R	R	F		R	R	R		R	R	R	R	R		R	R	R	R	R	R																
						QE 8.00	407	20	C	C	A	F	F	R	F	R	R	C		A	R	C	R	R			R	F	R	R	R																														
						QE 7.70	636	17	C	C	A	C	C	R	C	R		C		A	C	A	R	R			R	R		R																															

Abundance
VA; >10 species / field of view
A; 1-9 species / field of view
C ; 1 species /2-10 field of view
F; 1 species / 11-50 field of view
R; 1species / >51 field of view

(Continued)

Epoch	Age	Rock Unite	Martini (1971) NP Zones	Agnini et al. (2014)	NP biozones	QE Sample thickness	Abundance	diversity	*Coccolithus pelagicus*	*Ericsonia robusta*	*Ericsonia subpertusa*	*Thoracosphaera operculata*	*Thoracosphaera heimii*	*Thoracosphaera saxea*	*Zeugrhabdotus sigmoides*	*Cruciplacolithus primus*	*Cruciplacolithus intermedius*	*Cruciplacolithus tenuis*	*Micula decussata*	*Neochiastozygus sp.*	*Prinsius sp.*	*Ellipsolithus macellus*	*Neochiastozygus perfectus*	*Markalius inversus*	*Neochiastozygus eeosaepes*	*Ellipsolithus sp.*	*Neochiastozygus modestus*	*Chiasmolithus danicus*	*Cruciplacolithus edwardsii*	*Braarudosphaera bigelowii*	*Octolithus sp.*	*Lapideacassis sp.*	*Toweius pertusus*	*Lapideacassis asymmetrica*	*Pontosphaera sp.*	*Unknown species*	*Neochiastozygus imbriei*	*Chiasmolithus edentulus*	*Ellipsolithus distichus*	*Diantholitha mariposa*	*Discoaster sp.*	*Sphenolithus primus*
Paleocene	Danian	Dakhla Formation	NP4	CNP5	CNP5a	QE 7.40	701	17	C	C	A	C	C	R	C			C			VA	F	A	R	R			F		R		F		R	R					R	R	R
						QE 7.10	425	16	F	C	A	C			C			C		R	A	F	A		R			C				R	R		R		R					
						QE 6.80	938	15	C	C	A	C	C		C		R	C			VA	C	C		R		R	R									R					
						QE 6.50	456	17	C	C	A	C	F	R	F	R		C			A	C	C				R	C					R		R	R					
						QE 6.20	485	13	C	C	A	C		R	C			C		R	A	F	C		R								R								
						QE 5.90	481	16	C	C	A	C	F	R	C			C			A	F	A				R	R	R				R		R						
						QE 5.60	501	15	C	C	A	C	R	R	F	R		C		R	A	C	A					R				F								
						QE 5.30	935	13	C	A	A	C		R	C	R		C			VA	C	C					R				A								
						QE 5.00	516	13	C	C	A	C	R	R	C		R	C			A	C	C					R												
						QE 4.70	635	11	C	C	A	C			C			F			A	C	A					R	F											
						QE 4.40	684	16	C	C	A	C	R	R	F	R	F	C			A	C	C					F	R				R							
						QE 4.10	588	10	C	C	A	C			C			R			VA	C	A					F												
						QE 3.50	614	18	C	C	A	C	R	R	C		F	F		R	VA	A	C			R		R	R				R			R				
						QE 3.20	383	11	C	C	A	C	C		F			F			A	C	C					F												
						QE 3.00	630	13	C	C	A	C		R	C		F	C			VA	C	C					F								R				
						QE 2.90	364	12	C	C	A	C		R	C	R		C			A	C	C					R												
						QE 2.60	365	13	C	C	A	C	C		C	F	R	C			A	C	C					F												
						QE 2.30	526	12	C	C	A	C		R	C		R	C			A	C	A					F												
						QE 2.00	691	17	C	C	A	C	C	R	C		C	C			VA	A	A	R				C				R	R	R						
				CNP4	CNP4	QE 1.70	487	14	C	C	A	C	F	R	C		R	C			A	C	A					R				R							
						QE 1.40	606	16	C	C	A	C	F	R	C	F	F	C			A	C	A			R	R	F												
						QE 1.10	394	16	C	C	A	C	C	R	C	F	F	C			A	C	A	R			R	R												
						QE 0.80	410	12	C	C	A	C	F		C		C	C			A	C	C								R									
						QE 0.50	392	11	C	C	A	C	C		C		F	R			A	C	A																	
						QE 0.30	306	13	C	C	A	C	F	R	C		F	R			A	C	C								R									
						QE 0.15	353	13	C	C	A	C	C		C	F	R	F			A	C	C						R											
						QE 0.00	377	12	C	C	A	C	C		C			C		R	A	C	C							F										
						QE -0.02	338	13	C	C	A	C	C	R	C		R	F			A	C	C					R												
						QE -0.10	563	13	C	C	A	C	C		C	F	F	C			A	A	C					F												
						QE -0.50	468	13	A	C	A	C	C		C	R		C		R	A	C	C					R												
						QE -0.80	371	12	A	C	A	C	C		C	R	R	C			A	C	C																	
						QE -1.10	456	12	A	C	A	C	C		C	F	F	C			A	C	C																	
						QE -1.40	354	14	C	C	A	A	R	F	C	C	F	C			A	C	A					F												
						QE -1.70	554	14	A	C	A	C	F	R	C	F	F	C			A	C	C					F												
						QE -2.00	439	15	A	C	A	C	F	F	C	C	F	F		R		C	C	R				F												
						QE -2.25	420	15	C	C	A	C	F	R	C	R	R	F			A	C	C					R		R										
						QE -2.50	446	17	A	C	A	C	F	R	C	F	F	C			A	C	C	R			R	R	R											
						QE -2.80	474	15	A	A	VA	C	F		C	C	C	F		R	A	C	R			R		R												
						QE -3.20	591	14	A	C	A	C	C	R	C	C	F	F			A	C	C		R															
						QE -3.50	634	14	A	A	C	C	R	F	C	C	F	F			A	C	R	R																
						QE -4.00	450	15	C	C	A	C	F	R	C	F	R	C	R	R	A	F	C																	

6. Discussion

6.1. Calcareous Nannofossil Bioevents

Calcareous nannofossil bioevents had been adopted to delineate or approximate the LDE and the D/S boundary. *Chiasmolithus edentulus* is the earliest representative of *Chiasmolithus* taxa that have cross bars with median extinction line. The LDE distinct bed at the Tethyian region is commonly associated with the first entry of *C. edentulus* in the fossil record (Dinarès-Turell et al., 2010). It is also significant in the correlation among the Danish (the D/S boundary's type area), Spanish (Selandian's Global Stratotype Section and Point, GSSP), North Sea and Tethyan regions (Varol, 1989; Bernaola et al., 2009 and

Sprong et al., 2009). Agnini et al. (2014) viewed *C. edentulus* in Zone CNP5. Bernaola et al. (2009) documented that, the LO of *C. edentulus* at Zumaia (Spain) is ~10 m beneath Selandian's base and coincides the LOs of *Lithoptychius chowii* and *L. varolii*, as well as the first radiation of fasciculiths. Yet the *C. bidens* group occurs first at South Atlantic (Site 1262) and Qreiya (Egypt) (Monechi et al., 2013). In Tunisia, *C. edentulus* first appears in coincidence with the appearance of small fasciculiths (*L. chowii*, *L. felis*, etc.), the first radiation of fasciculiths, and the LCtO of *Pontosphaera* sp. Sprong et al. (2009, 2011, 2013) observed that the LOs *C. edentulus* small *Fasciculithus* (*L. chowii*) at Qreiya are coincident and is approximately 1.2 m below the LDE. Kasem et al. (2017) observed the coincidence of the LOs of *C. edentulus*, *Diantholitha* sp., *L. felis*, and *L. schmitzii* at Misheiti (Sinai, Egypt). Kasem (2016) noted that *C*. *edentulus* first appears in coincidence with the LOs of *Lithoptychius felis, L. varolii*, and *L. schmitzii,* which are followed by the appearance of *Diantholitha* sp., *L. chowii, L. collaris*, and *L. vertebratoides* at north Wadi Qena (Eastern Desert, Egypt). However, *C. edentulus* appears in coincidence with the LOs of *L. vertebratoides*, *L. felis*, *Diantholitha* sp., and *L. schmitzii* at Gunnah (Farafra Oasis, Western Desert, Egypt). Kasem et al. (2022) noted that the LO of *C*. *edentulus* coincides with the LO of *D. magnolia* at Nezzazat (Sinai, Egypt) and occurs in the LDE bed, just overhead the LOs of *D. mariposa, D. alata, L. felis, L. varolii,* plus *L. collaris*. Kasem (2023) noted that the LO of *C*. *edentulus* coincides with the LO of *S. primus* that is continuous from the beginning of its range at Nukhul (Sinai, Egypt). In this study, *C. edentulus* first occurs in sample QE 7.70, about 1.47 m below the LDE marker beds (Fig. 3); whereas, genera *Diantholitha* and *Lithoptychius* appear in sample QE 8.30 (87 cm below the LDE marker beds, Fig. 3) and represent the first radiation of *Fasciculithus*. The LCtO of *Pontosphaera* sp. was recorded in sample QE7.10, 60 cm below the LO of *C. edentulus* (Fig. 3).

The LO of *Sphenolithus primus* was regarded significant bioevent in stratigraphy (Quillévéré et al., 2002). However, early occurrences of this taxon are very scarce and discontinuous (see Kasem et al., 2017 for references). Moreover, the LO of *Sphenolithus* is diachronus with respect to the LO of *Fasciculithus* and paleomagnetic polarity (Fuqua et al., 2008). The first appearance of *S. primus* was viewed either in Varoli's (1989) Subzone NTp5c-NTp6, Subzone NTp7a, or in Subzone NTp7b (Arney and Wise, 2003, and Monechi et al., 2013).

Furthermore, the precise LO of *S. primus* is unrecognizable because of the presence of forms intermediate between *Sphenolithus* and *Octolithus* (Agnini et al., 2007). As such, the LCtO of *S. primus* is considered a significant bioevent in place of its LO (Kasem et al., 2017). *Sphenolithus primus* appears with continuous occurrence at ~ 5.8 m above its first occurrence at Zumaia (Bernaola et al., 2009). In Tunisia *S*. *primus* first appears at ~ 8 m overhead the LDE bed (Sprong et al., 2013). Yet *S. primus* at Qreiya was viewed ~ 2.4 m overhead the D/S boundary (LDE herein) (Monechi et al., 2013). Thus, the LDE occurs in between the LO and LCtO of *C. edentulus* and *S. primus*, respectively. In this study, the LO of *S. primus* occurs at 4 m below it LCtO (Fig. 3). The first appearances of *C. edentulus* as well as *S. primus* occurs at about 1.77 m and 1.47 m below the LDE bed, respectively; however, *S. primus*' LCtO appears at 1.92 m overhead the LDE bed's top (Fig. 3). At Nezzazat (Sinai, Egypt), Kasem et al. (2022) noted that the early occurrences of *S. primus* are rare and discontinuous and above the first appearances of *Diantholitha* sp., *Lithoptychius chowii*, *L. felis*, *L. collaris*, *L. schmitzii*, and *L. varolii*. Kasem (2023) suggested a hiatus represent the uppermost Danian at Nukhult area (Sinai, Egypt).

Diantholitha is a remarkable bioevent in the late Danian (Aubry and Salem, 2013a, b). Kasem et al. (2017) noted that at Misheiti (Sinai, Egypt), *D. magnolia* and *D. mariposa* co-occur, and then *D. alata* occurs later as found at Zumaia (Spain) (Monechi et al., 2013). However, *D*. *mariposa, D. magnolia* and *D. alata* first occur together in North Wadi Qena (Eastern Desert, Egypt) and Gunnah (Western Desert, Egypt) (Kasem, 2016). *Diantholitha* was recorded below the occurrence of the *Chiasmolithus edentulus* in sections in South Atlantic, Spain and Egypt (Monechi et al., 2013). Kasem et al. (2017) observed that *Diantholitha*' LO is coincident with the LO of *C. edentulus* at Misheiti (Sinai, Egypt). Similar finding was noted at Gunnah (Western Desert, Egypt, Kasem, 2016). At North Wadi Qena (Eastern Desert, Egypt), *Diantholitha* occurs directly above the LOs of *Lithoptychius* sp. (Kasem, 2016).

Lithoptychius appears after appearance of *Diantholitha* (Kasem et al., 2017). However, Kasem (2016) noted that the former species precedes *Diantholitha*' LO of at North Wadi Qena (Eastern Desert, Egypt). At Zumaia, first appearance of *Lithoptychius* coincides the appearance of *C. edentulus.* Similar findings were noted at Misheiti, North Wadi Qena and Guna, Egypt (Kasem, 2016 and Kasem et al., 2017). However, Monechi et al. (2013) mentioned that at Walvis Ridge (Site 1262, South Atlantic) and Qreiya (Egypt), *C. bidens* group precedes *C. edentulus* in appearance. The LOs of *Lithoptychius* is coincident with the LO of *C. edentulus*. In this study, first appearances of *Diantholitha* and *Lithoptychius* are coincident (Table 1 and Fig. 4).

The frequency patterns of fasciculiths show several radiations in this genus (Bernaola et al., 2009). The earliest one is close to the LDE; whereas the younger episode occurs near the topmost of the Paleocene (Schmitz et al., 2011). Bernaola et al. (2009) relied on the LO of *Diantholitha mariposa* to delineate the first radiative event of fasciculiths at Zumaia, somewhat beneath the LO of *Chiasmolithus edentulus*. A similar finding was recorded at the ground of LDE bed in Tunisia and somewhat below it in Egypt (e.g., Guasti et al., 2006; Sprong et al., 2009, and Bernaola et al., 2009; this study). Steurbaut and Sztrákos (2008) marked this episode by the LOs of small *Fasciculithus* species that include *Diantholitha* sp., and *Lithoptychius* sp. However, Monechi et al. (2013) viewed *Diantholitha* sp. below *Lithoptychius* sp. A new species, *L. schmitzii,* was recognized by Monechi et al. (2013) in the

range of *L. chowii* and *L. varolii*. They recommend using it as a marker to the first radiation of fasciculiths when other *Lithoptychius* taxa are missing. Monechi et al. (2013) documented that the radiations of *Fasciculithus* during late Danian are disconnected by a free of *Fasciculithus* interval (Bernaola et al., 2009). And within this interval, the abundances of *Sphenolithus primus*, *Toweius* sp. and *Zeugrhabdotus sigmoides* markedly increase. Kasem et al. (2017) relied on the LOs of *Lithoptychius* sp. and/or *Diantholitha* spp for delineation of the first radiative event of fasciculiths, which coincides the entry of *C*. *edentulus*. In this research, this radiation is delineated by first appearance of genera *Diantholitha* - *Lithoptychius* (sample QE 8.30, Fig. 4), which are coincident but occur 60 cm above the LO of *C. edentulus* (Figs.3, 4, and Table 1). Kasem et al. (2022) reported that the first representative of fasciculiths at G. Nezzazat (Sinai, Egypt) is marked by the LO of *Lithoptychius schmitzii* at about 5.05 m beneath the marker bed of the LDE, and the radiation of fasciculiths followed it, where *Diantholitha* sp. and *Lithoptychius* sp. occurs in the LDE bed's base. Kasem (2023) reported that *Diantholitha*, early representatives of *Lithoptychius* are absent at Nukhul (Sinai, Egypt) suggesting a hiatus in this interval.

At Zumaia in Spain, Bernaola et al. (2009) suggested the LO of *Lithoptychius ulii* to delineate the second radiative episode of fasciculiths. Kasem et al. (2017) marked the second radiation of fasciculiths at Misheiti (Sinai, Egypt) by the coincident first appearances of *L. billii*, *L. ulii,* and *L. pileatus*. Kasem et al. (2022) reported that at G. Nezzazat, the LO of *L*. *ulii* was viewed about 0.3 m beneath Zone NP5. They also noted coincident lowest ocurrences of *L. billii, L*. *ulii, L. janii,* and *L. stegostus;* however, *L*. *ulii* had to appear earlier (Varoli, 1989 and Monechi et al., 2013). Kasem (2023) reported that the LOs of *L. ulii* coincides with the first appearance of *F. tympaniformis* at Nukhul (Sinai, Egypt). In this study, this second radiative episode is traced at the coincident lowest occurrences of *L. billii* and *L. ulii* at about 5.7 m above the first radiative episode (Figs. 3, 4 and Table 1).

Braarudosphaera were viewed with common occurrence up to the base of Selandian at Zumaia (Spain), at or roughly above the 2nd radiative episode of fasciculiths (Schmitz et al., 2011). Yet *B. bigelowii* is scarce and sporadic in the Tethyan sections (Kasem et al., 2022 and 2023, this study, Table 1).

Prinsius spp. dominates the base of the LDE interval, as documented by Monechi et al., (2013). It has its peak abundance in the midst portion of the LDE bed. Kasem (2016), the abundance of *Prinsius* spp. reaches its maximum within Zone NP4 at the Misheiti, North Wadi Qena, and Gunnah sections in Egypt. In this study, *Prinsius* spp. reached its maximum (82.9 % of the total assemblage) in sample QE 9.22 (Table 1), at about 5 cm overhead the LDE bed's base (Fig. 3), whereas sample QE 9.17 that represent the LDE's base is free of *Prinsius* spp. (Table 1).

Calcareous nannofossil's diversification reveal remarkable variation throughout the LDE; where it drops from 24 species below the LDE bed to 2 species in the basal sample (QE 9.17) of the LDE bed and increases to 22 species in the LDE bed's top (Table 1, Fig. 4). Similarly, the frequency of calcareous nannofossils reached its minimum (2 individuals) in the basal sample of the LDE (QE 9.17) (Table 1, Fig. 4).

a. The LDE

Selandian's base in Egypt was traced at a distinct organic-rich, shale bed's base in the Dakhla Formation (e. g., Obaidalla et al. 2009; Sprong et al., 2009, 2011; Youssef, 2009; Aubry et al., 2012, and Kasem et al., 2022). Later, it was noted that this distinct bed occurs under the Selandian's base (Schmitz et al., 2011), and this distinct bed had been referred to as the LDE bed. The LDE was recorded at Zumaia (Spain), which has the base of Selandian's GSSP (Bernaola et al., 2009). It coincides with a lithological change; ~ 10 m below the base of Selandian (Schmitz et al., 2011). This event occurs in Jordan; Tunisia; ODP sites and North Sea Basin (Guasti et al., 2005; Steurbaut et al., 2000; Guasti et al., 2006; Westerhold et al., 2008; Sprong et al., 2013, and Kasem et al., 2022).

The LDE in Egypt is mostly represented by a basal bed with no benthic foraminifera and planktonic foraminifera have low-diversity in it (Sprong et al., 2011), underlain by a carbonate-poor interval with a sharp and possibly unconformable contact between them (Speijer, 2003b). This carbonate poor interval is sometimes included in the LDE (Soliman and Obaidalla, 2010), and at times were not included in it (Sprong et al., 2011).

In Tunisian sections, the LDE is a glauconitic marker bed (Sprong et al., 2009), and the lithological and benthic foraminiferal changes that characterize this interval in some Egyptian sections are missing (Sprong et al., 2013). Lithological changes, $\delta^{13}C$ excursion, and biotic assemblages indicate that this episode is a global warming event (Westerhold et al., 2011). Yet the $\delta^{13}C$ excursions, as documented by Sprong et al. (2013) in Tunisia and in Qreiya, as documented by Aubry et al., 2012, do not support this hypothesis. Kasem et al. (2017) traced the LDE at Misheiti (Sinai) based on abrupt negative $\delta^{13}C$ excursions. Similar finding was recorded at North Wadi Qena (Eastern Desert, Egypt) and Gunnah (Western Desert, Egypt, Kasem, 2016). Similarly, the $\delta^{18}O$ values abruptly decrease during the LDE at Misheiti and North Wadi Qena; however, the $\delta^{18}O$ values unusually increase at Gunnah (Kasem, 2016). A remarkable drop in carbonate content was noted in the LDE interval in these sections (Kasem, 2016 and Kasem et al., 2017). Isotopic data documented by Aubry et al. (2012) reveal that the LDE bed's basal sample (QE 9.17) is free of calcite, however $\delta^{13}C_{carb}$ increases into 2.02 ‰ in sample QE 9.32, about 15 cm above the LDE bed's base (Fig. 5). Furthermore, $\delta^{18}O_{carb}$ at Qreiya reached 5.30 ‰ in the LDE bed's top (Fig. 5). These isotopic outcomes do not support hyperthermal episode during the LDE interval (Aubry et al., 2012).

b. The D/S boundary

Selandian's initial type locality located in Denmark, where a hiatus characterized the D/S transition (Clemmensen and Thomsen, 2005). Subsequently, various studies attempted to re-define the GSSP for the Selandian (see references in Kasem et al., 2017), which was formally chosen at Zumaia in Spain (Schmitz et al., 2011).

The placement of this boundary is intricate on account of the lack or scarcity of the biozones' marker taxa across this interval (Sprong et al., 2009). At Zumaia, it was placed in Zone NP4 based on the lowest common occurrence of taxon *Braarudosphaera bigelowii*, in concurrence with the lithological change (Schmitz et al., 2011). In its type locality, this limit was positioned based on the lithological change at the NP4/NP5 Subzonal boundary (Clemmensen and Thomsen, 2005). In Egypt, this limit was placed either at the beginning of Zone NP5; Zone P3 (within Zone's NP4 middle part); at the appearance of *Fasciculithus*; at the appearance of *Diantholitha mariposa* in Subzone NTp8c; at the first appearances of *Sphenolithus primus* and *Fasciculithus* sp.; at the top of a major negative $\delta^{13}C$ excursion (see Kasem et al., 2017 for references). At Zumaia, the LO of *Lithoptychius ulii* (base of 2nd radiation of fasciculiths) is the preferable bioevent delineate the D/S boundary globally (Schmitz et al., 2011). The LO of *L. ulii* at Zumaia (Spain) occurs ~ 0.20 m beneath Selandian's base, and *F. tympaniformis* appears ~ 1.1 m overhead it (Schmitz et al., 2011). Consequently, the Selandian's base can be traced in between these two bioevents. Therefore, the base of Selandian in this study is tentatively traced within Zone CNP7 (Fig. 3).

At Qreiya, Sprong et al. (2011) relied on the first appearances of *Lithoptychius ulii* plus *L. billii* to delineate the entry of Varoli's (1989) Subzone NTp8b, at ~ 0.5 m above the marker bed of the LDE. They traced the base of Selandian in this interval. Kasem et al. (2017) delineated Selandian's base at Misheiti (Sinai, Egypt) within Zone NP4 based on sudden drop in $\delta^{13}C$ and $\delta^{18}O$ values as well as carbonate content without any lithological change across this boundary. Kasem et al. (2022) traced Selandian's base at G. Nezzazat (Sinai, Egypt) at Zone's NP4 top, at abrupt decrease in the calcareous nannofossils' abundance. Kasem (2023) sited this boundary at Zone's NP5 base and suggested unconformity at this boundary. In this study, the uppermost 4 m of the study interval are assigned to the Danian-Selandian interval (Fig. 3).

6.2. Paleoecology

Calcareous nannofossils are sensitive to environmental changes and their vertical and horizontal distributions are controlled in modern oceans by water temperature and nutrient availability and other ecological factors (Winter et al., l994; Bralower, 2002; Bornemann, 2003, and Bernaola et al., 2007). Thus, they provide information on palaecological changes of their living area throughout the geologic time. Several previous studies provided information about the ecological factors controlled the distribution of calcareous nannofossils (see Bralower, 2002, Bernaola et al., 2007 and Kasem et al., 2022 for more references). The calcareous nannofossil taxa that have known paleotemperature preferences and paleofertility affinity are summarized in Table 2.

Table 2 shows the ecological preferences of selected calcareous nannofossil taxa recognized in this study

Warm-water Forms	*Coccolithus pelagicus*, *Ericsonia subpertusa*, *Thoracosphaera operculata*, *T. saxea*, *Braarudosphaera* sp., *Sphenolithus* sp., *Fasciculithus* sp., *Discoaster* sp., and *Pontosphaera* sp.
Cool-water Forms	*Markalius inversus*, *Cruciplacolithus* sp., *Zeugrhabdotus sigmoides*, *Chiasmolithus* sp., *Prinsius* spp., *Neochiastozygus sp.*
Cosmopolitan Forms	*Micula decussata*, *Toweius pertusus*
Oligotrophic Taxa	*Discoaster* sp., *Fasciculithus* sp., *Octolithus* sp., *Sphenolithus* sp.
Eutrophic Taxa	*Zeugrhabdotus sigmoides*, *T. saxea*, *Neochiastozygus* sp.
Mesotrophic taxa	*Cruciplacolithus* sp., *Prinsius* spp.

Prinsius spp. is generally regarded as cold-water, a nutrient-rich indicator (Haq et al., 1976; Wise and Wind, 1977, and Bernaola et al., 2007). However, some authors regarded it a mesotrophic taxon (Agnini et al., 2007; Mutterlose et al., 2007, and Bernaola et al., 2007). *Ericsonia subpertusa* was considered as warm-water taxa by several authors (Agnini et al., 2007, and Bown and Pearson, 2009) and prefer oligotrophic conditions (Bralower, 2002, and Bernaola et al., 2007).

Thoracosphaera is a warm-water taxon (Bassiouni et al., 1991). *Thoracosphaera saxea* has been regarded as a high fertility taxon (Thibault and Gardin, 2007). *Zeugrhabdotus* has been regarded as a high- to mid-fertility and cold-water taxon (Eshet and Almogi- Labin, 1996). *Zeugrhabdotus sigmoides* was regarded as a cool-water taxon by several authors (Pospichal and Wise, 1990). *Markalis inversus* was considered as a cool-water form (Bassiouni et al., 1991). *Cruciplacolithus* is regarded as a cool-water taxon (Abdel Hameed and Faris, 1984), and adapted to mesotrophic settings (Aubry, 1998 and Fuqua et al., 2008). *Chiasmolithus* has been regarded as taxon prefer cold-water environments (Bralower, 2002), adapted to mesotrophic - eutrophic water (Aubry, 1998,

and Tremolada et al., 2007). However, Fuqua et al. (2008) regarded it as an oligotrophic indicator. *Neochiastozygus* indicates mesotrophic conditions (Gibbs et al., 2006). The paleoecological affinities of *Sphenolithus* are not well-known (Fuqua et al., 2008). However, this genus has close association with *Discoaster*, which prefers warm, oligotrophic conditions (Wei and Wise, 1990; Aubry, 1998; Agnini et al., 2006, and Fuqua et al., 2008). In addition, it decreases when high-latitude and more eutrophic *Prinsius martinii* increases (Haq and Lohmann, 1976). Agnini et al. (2006) concluded that the nutrients availability is the main controller of this taxon's abundance and distribution. The ecological affinities of *Fasciculithus* group (including *Diantholitha* and *Lithoptychius*) is difficult to recognize (Mutterlose et al., 2007), however, their great size and robust form indicate a deep habitat (Fuqua et al., 2008). The close association of this taxon with *Discoaster* indicates that it prefers warm and oligotrophic environments (Gibbs et al., 2006; Bernaola et al., 2007, and Fuqua et al., 2008).

Calcareous nannofossils counts suggest mesotrophic and cool-water conditions prevailed during most of the study interval (Fig. 5). However, warm-water taxa dominate the assemblage in samples QE -3.5 to sample -0.02. In addition, the warm-water taxa represent 100% of the whole taxa in the basal sample of the LDE bed (QE9.17) and at about 85 cm above the LDE bed's base (Fig. 5). *Prinsius* and *Ericsonia subpertusa* are the major components of calcareous nannofossil assemblages during the study interval (Fig. 5). Both show negative correlation during the study interval (Fig. 4).

Also, Figure 6 discriminated the affinities of the investigated taxa into three groups (I, II, and III) with their characteristic calcareous nannofossil assemblages. Group I is dominated by high occurrence of the cool-water taxa *Prinsius* spp., and *N. perfectus*, while group II is characterized by high percentages of the warm-water taxa *E. subpertusa*, *E. robusta*, *T. operculata*, *C. pelagicus*, and *E. macellus*. Group III is populated by calcareous nannofossil assemblage comprises *S. primus*, *C. edentulus*, *T. pertusus*, *C. danicus*, *T. heimii*, and *C. intermedius*. Figure 7 illustrates the samples distribution based on the calcareous nannofossil contents. The left quarters signify the samples inhabiting by calcareous nannofossil that are flourished in the eutrophic conditions and open marine signatures and highly populated by cool-water taxa (e.g., *Prinsius* spp.). On the other hand, the samples occupy the right quarters encompasses the oligo-mesotrophic conditions of the nearshore environments that are inhabited by high occurrence of warm -water taxa (most of group II). Accordingly, most of the investigated samples are constituted higher percentage of the cool-water taxa, except the lowermost interval which dominated by warm water taxa (Fig. 7).

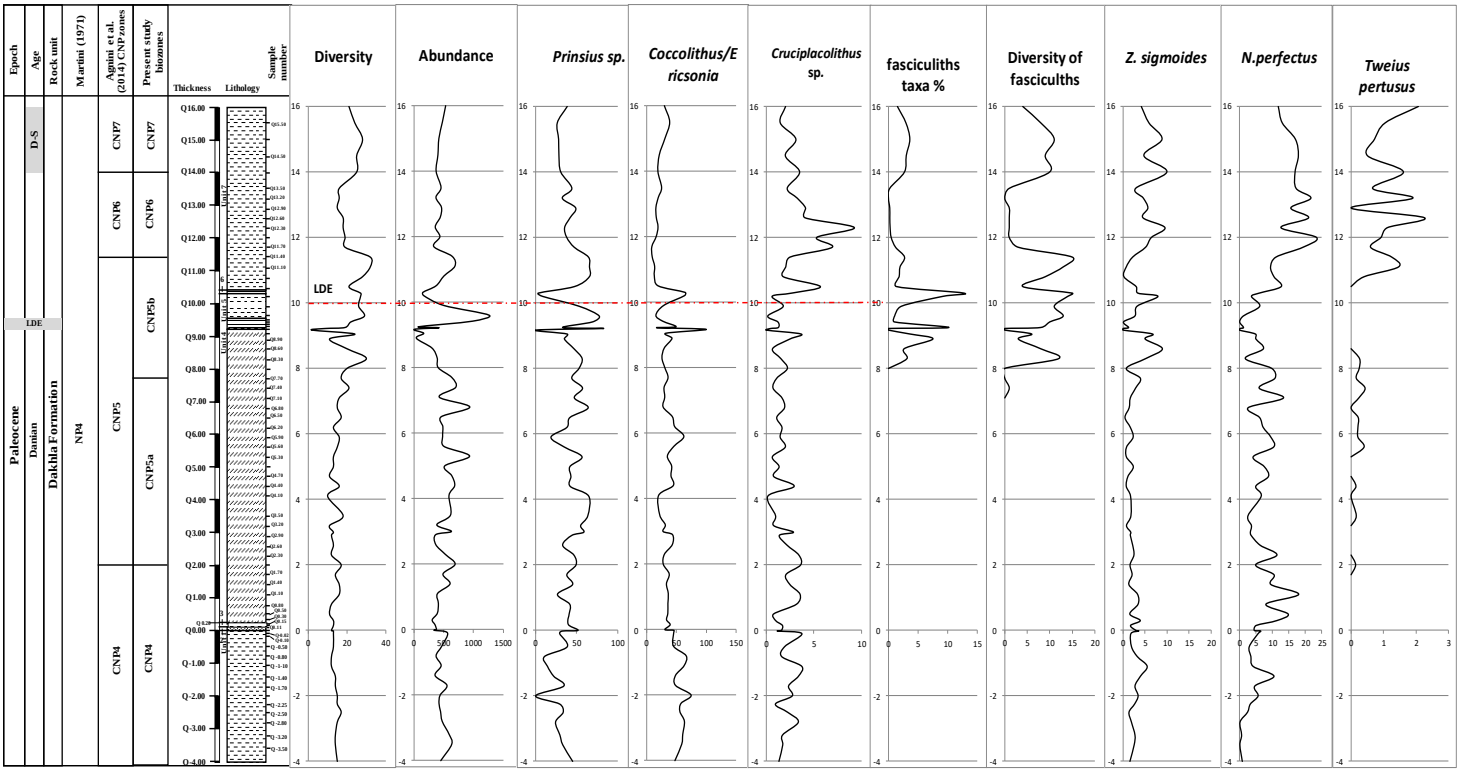

Fig. 4: shows calcareous nannofossils' diversity and total abundance as well as abundances of selected taxa at the Qreiya section, east Qena, Eastern Desert, Egypt

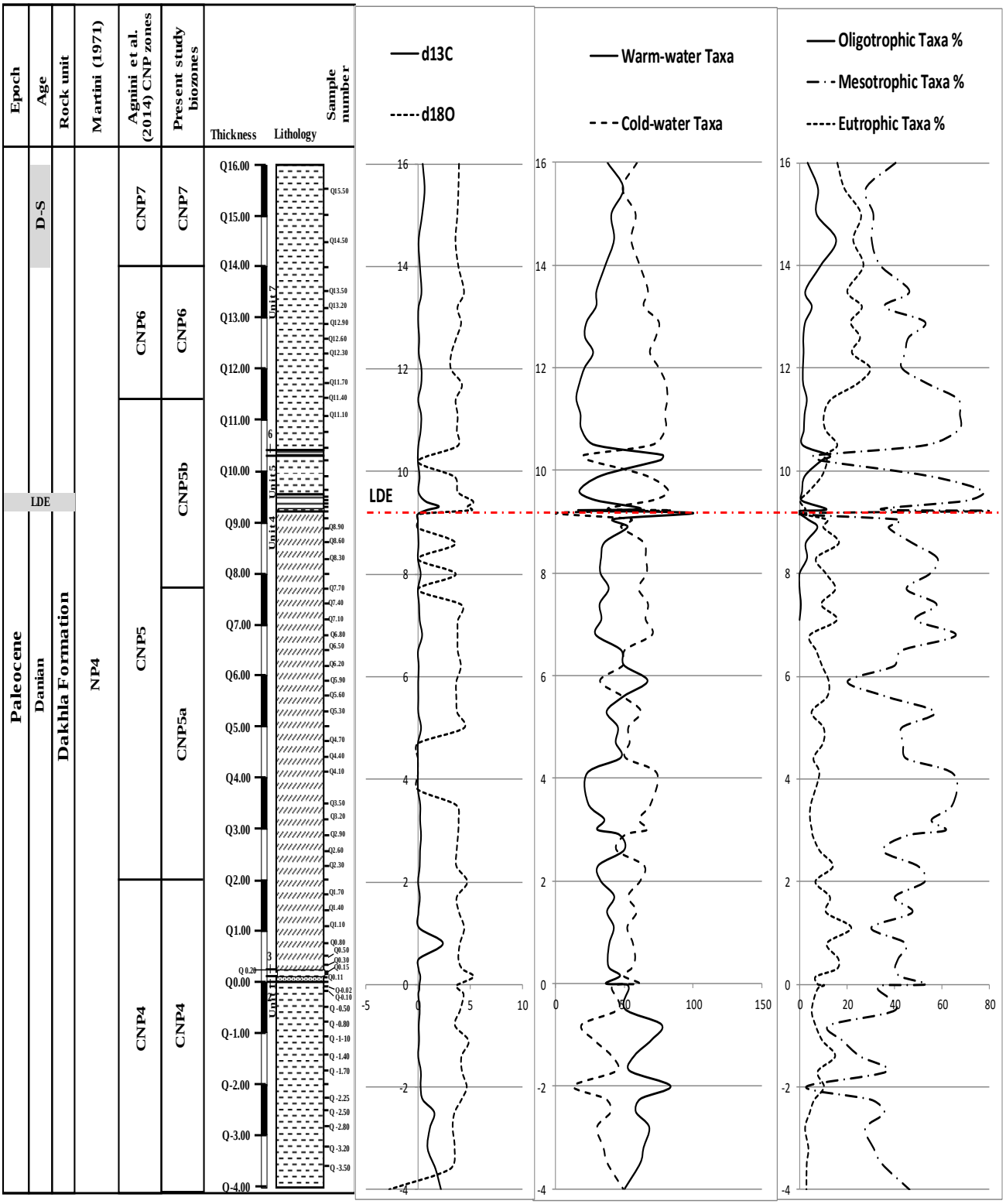

Fig. 5: shows $\delta^{13}C$ and $\delta^{18}O$ variations (re-drawn depending on measurements of Aubry et al., 2012), abundances of cold-water, warm-water, oligotrophic, mesotrophic and eutrophic taxa at the Qreiya section, east Qena, Eastern Desert, Egypt

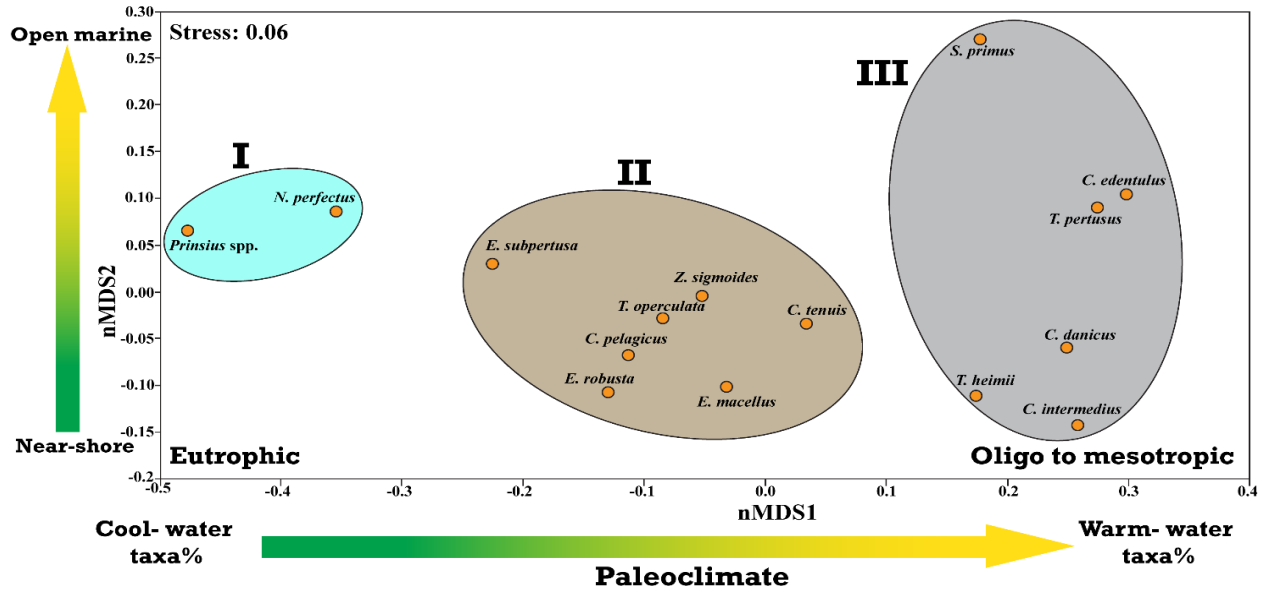

Fig. 6: R-mode nMDS chart for the investigated calcareous nannofossil of the Qreiya section, east Qena, Eastern Desert, Egypt

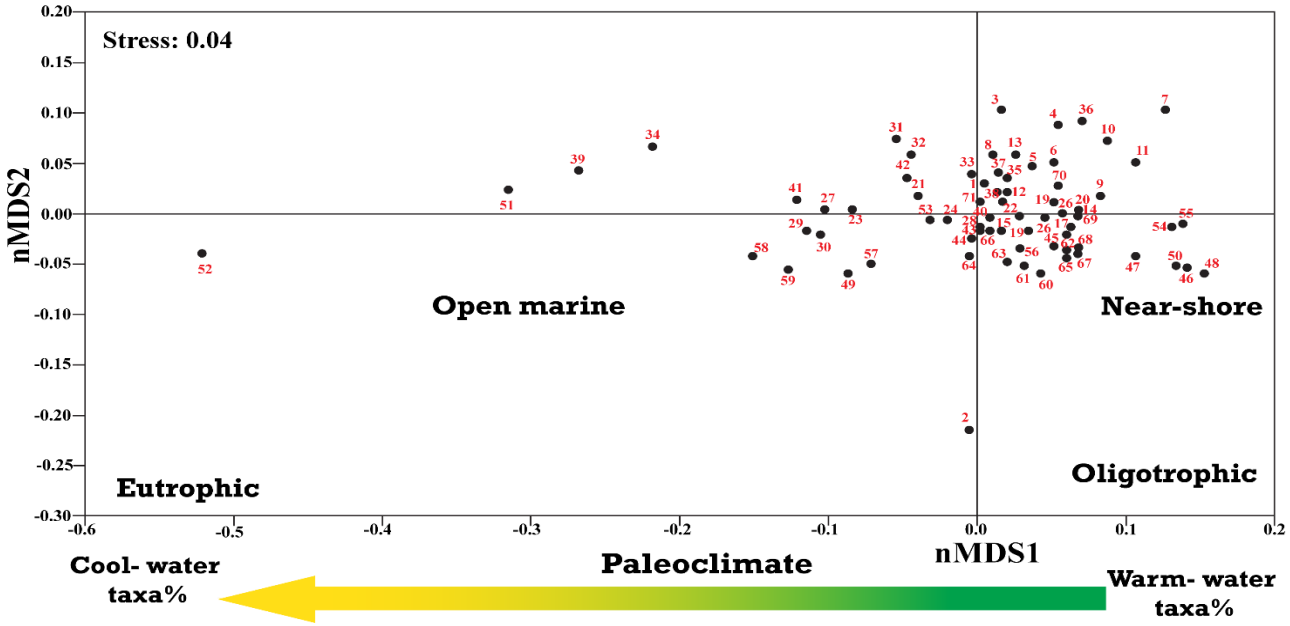

Fig. 7: Q-mode nMDS for the investigated calcareous nannofossil of the Qreiya section, east Qena, Eastern Desert, Egypt

Summary

Variations in Danian - Selandian calcareous nannofossils were revealed at the Qreiya section. Lithostratigraphically, the studied interval belongs to the Dakhla Formation. Four calcareous nannofossil zones had been delineated (CNP4, CNP5, CNP6 and CNP7). Zone CNP5 had been divided on the basis of the LO of *Chiasmolithus edentulus* into Subzones CNP5a and CNP5b. The bistratigraphic importance of significant calcareous nannofossils taxa were discussed in this work. *Chiasmolithus edentulus* first occurred at about 1.47 m below the LDE marker bed; however, *Diantholitha* sp. and *Lithoptychius* sp. appear at about 87 cm below this distinct bed. They mark the first radiative episode of *Fasiculthus*. *Sphenolithus primus* first occurred at 4 m below its lowest continuous occurrence and the LDE bed occurs in between these two bioevents (about 1.77 m above the LO and 1.92 m below the LCtO). *Diantholitha* and *Lithoptychius* appear at the same level in this study and mark the first radiation of *Fasiculthus*. About 5.7 m is between this radiative episode and the second episode (LO of *L. ulii*). *Braarudosphaera bigelowii* is scarce and sporadic in the study interval. Calcareous nannofossils' diversity and frequency show remarkable change across the LDE. *Prinsius* spp. reached its maximum at about 5 cm above the LDE bed's base, yet the basal sample of this bed is free of this taxon. Several suggested to be new species belongs to *Diantholitha* and *Lithoptychius* has been recognized in the study interval. The D/S boundary is suggested to be in Zone CNP7. Calcareous nannofossil

counts revealed prevalence of mesotrophic and cool-water taxa during most of the study interval. However, warm-water taxa dominate the assemblage in the study interval's lower part. They also dominate the LDE basal sample and at about 85 cm above the base of the LDE bed. *Prinsius spp.* and *Ericsonia subpertusa* are the major constitutes of the assemblages. They have negative correlation during the study interval. A more detailed study is recommended on the suggested new *Diantholitha, Lithoptychius, Pontosphaera* and *Lapideacassis species*, which are identified in this study.

Acknowledgement

Our warm appreciation and gratitude are to Prof. Dr. Mamdouh Soliman and Prof. Dr. Nageh Obaidalla (Department of Geology, Assiut University), Late Prof. Dr. Robert Knox (British Geological Survey), and Prof. Birger Schmitz (Lund University, Sweden) for their fieldwork, description and collecting the samples of this study.

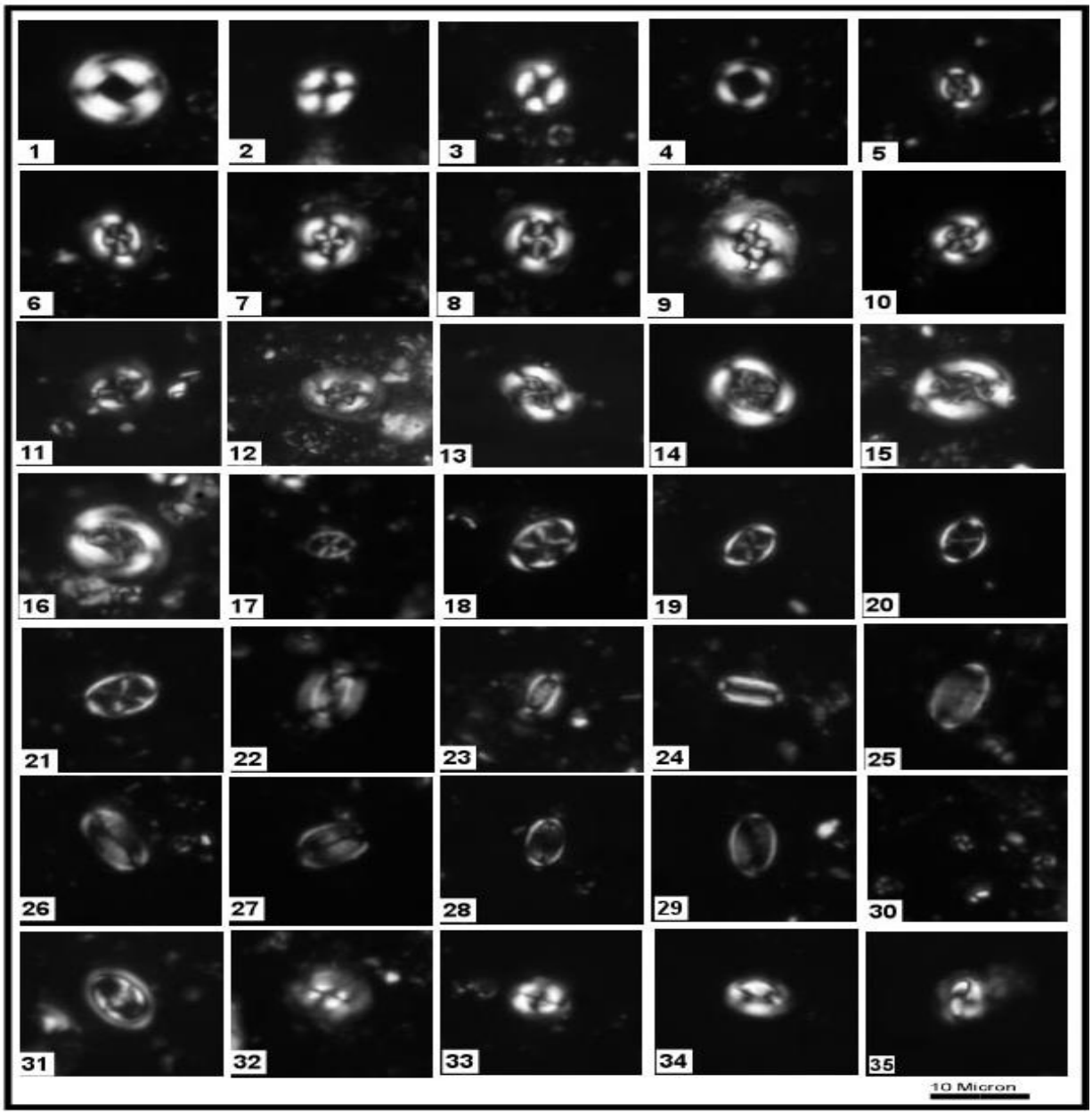

Plate 1

1 *Ericsonia subpertusa.* Sample QE 10.80, Subzone CNP5b. 2, 3 *Coccolithus pelagicus*. 2, sample QE 9.90; 3, sample QE 8.00, Subzone CNP5b. 4 *Ericsonia robusta*. Sample QE 8.60, Subzone CNP5b. 5 *Cruciplacolithus primus*. Sample QE 8.00, Subzone CNP5b. 6, 7 *Cruciplacolithus intermedius*. Sample QE 10.30, Subzone CNP5b. 8 *Chiasmolithus danicus*. Sample QE 8.00, Subzone CNP5b. 9 *Cruciplacolithus tenuis*. Sample QE 14.50, Zone CNP7. 10-12 *Chiasmolithus consuetus*. 10, sample QE 11.40, Zone CNP6; 11 sample QE 15.00; 12 sample QE 15.50, Zone CNP7. 13, 14 *Chiasmolithus edentulus*. Sample QE 16.00, Zone CNP7. 15, 16 *Chiasmolithus bidens*. 15 sample QE 15.50; 16 sample QE 15.00, Zone CNP7. 17 *Neochiastozygus eosaepes*. Sample QE 6.20, Subzone CNP5a. 18-21 *Neochiastozygus*

perfectus. 18, 20 sample QE 11.70, Zone CNP6; 19, 21, sample QE 10.30, Subzone CNP5b. 22 *Ellipsolithus macellus.* Sample QE 7.10, Subzone CNP5a. *23 Ellipsolithus distichus*. Sample QE 8.00, Subzone CNP5b. *24 Ellipsolithus* sp. Sample QE 1.40, Zone CNP4. 25-29 *Pontosphaera* sp. 25, 27 sample QE 10.80; 26, 28, sample QE 11.10; 29 sample QE 10.30, Subzone CNP5b. *30 Prinsius* spp. Sample QE 5.90, Subzone CNP5a. 31 *Zeugrhabdotus sigmoides*. Sample QE 9.90, Subzone CNP5b. 32 *Markalius inversus*. Sample QE 7.40, Subzon CNP5a. *33-35 Toweius pertusus*. 33 sample QE 11.10, Subzone CNP5b; 34 sample QE 16.00, Subzone CNP5a; 35 sample QE 15.00, Zone CNP7.

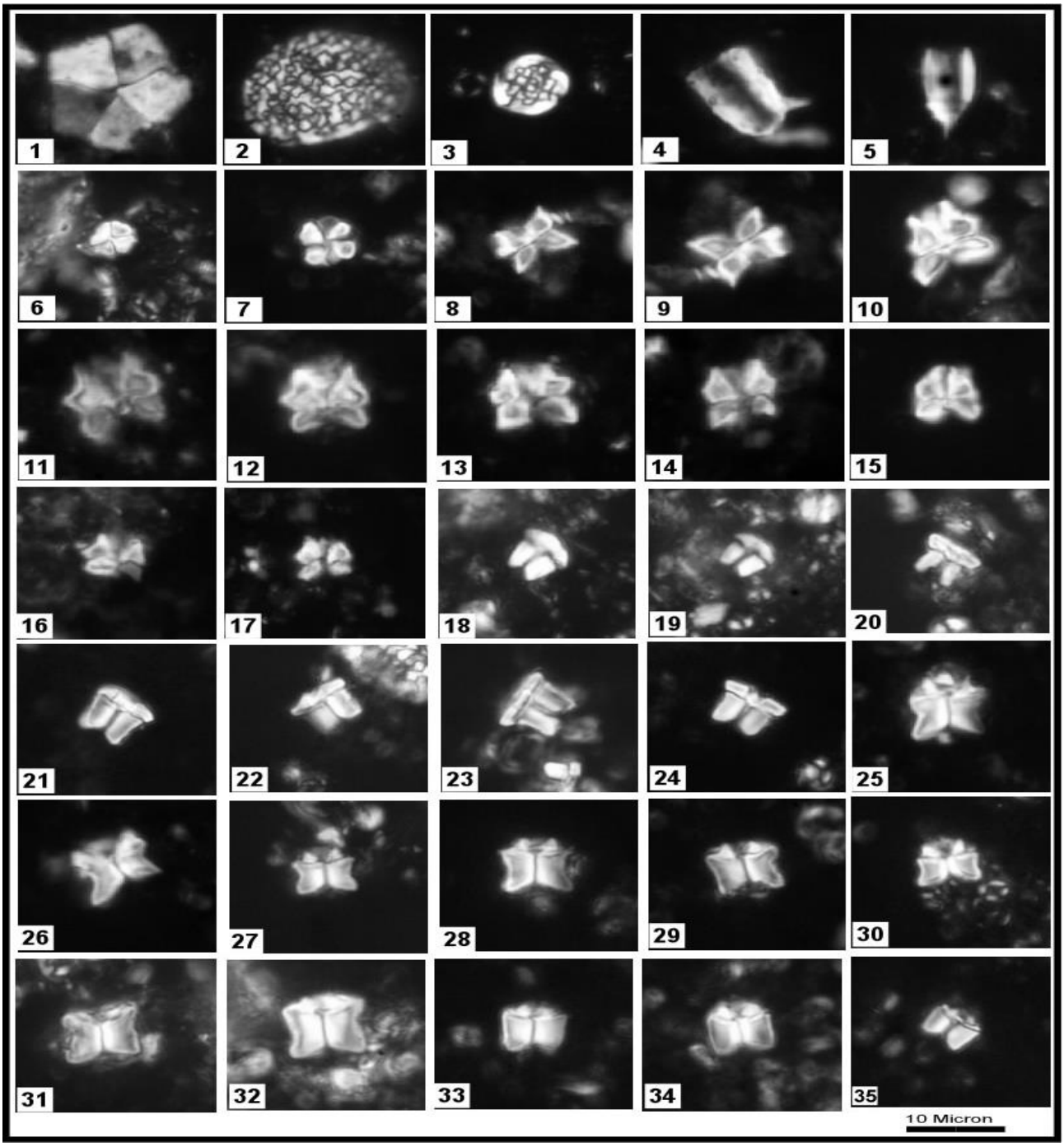

Plate 2

1 *Braarudosphaera bigelowii*. Sample QE 9.60, Subzone CNP5b. 2 *Thoracosphaera operculata*. Sample QE 11.10, Subzone CNP5b. 3 *Thoracosphaera saxea. Sample* QE 11.10, Subzone CNP5b. 4 *Lapideacassis* sp. Sample QE 5.30, Subzone CNP5a. 5 *Lapideacassis asymmetrica.* Sample QE 2.00, Subzone CNP5a. 6 *Octolithus* sp. Sample QE 15.00, Zone CNP7. 7 *Sphenolithus primus* sample QE 15.00, Zone CNP7. 8, 9 *Diantholitha mariposa*. Sample QE 10.30, Subzone CNP5b. 10-15 *Diantholitha magnolia*. 10, sample QE 9.90, 11, 13 sample QE 8.90, 4 sample QE 9.22; 15 sample QE 9.60, Subzone CNP5b. 16, 17 *Diantholitha alata*. 20 sample QE 8.30, Subzone CNP5b. 18, 19 *Lithoptychius janii*.

Sample QE 15.50, Zone CNP7. 20-24 *Lithoptychius stonehengii*. 20, 21, 23 sample QE 16.00; 22 sample QE 15.50, Zone CNP7; 24 sample QE 10.20, Subzone CNP5b. 25, 26 *Lithoptychius vertebratoides*. Sample QE 10.30, Subzone CNP5b 27-30 *Lithoptychius chowii.* 27 sample QE 15.00; 28 sample QE 14.50; 29 sample QE 15.50, Zone CNP7; 30 sample QE 11.10, Subzone CNP5b. 31, 32 *Lithoptychius billii*. 31 sample QE 15.50; 32 sample QE 15.00, ZoneCNP7. 33-35 *Lithoptychius ulii.* Sample QE 15.00, Zone CNP7.

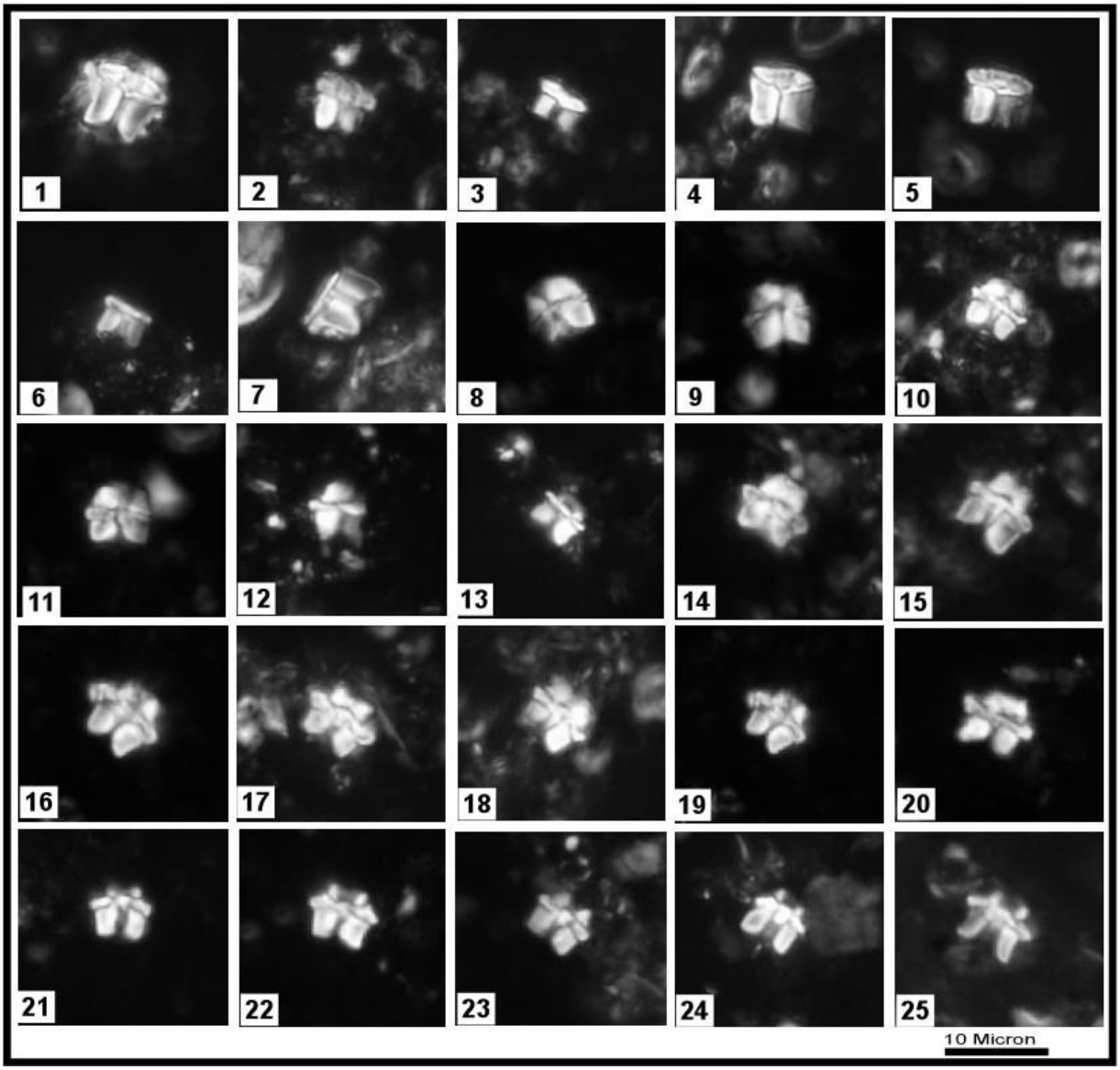

Plate 3

1, 4, 5 *Lithoptychius pileatus*. 1, 5 sample QE 16.00; 4 sample QE 15.50, Zone CNP7. 2, 3, 6, 7 *Lithoptychius stonehengii.* 2, sample QE 16.00; 2, 3 sample QE 15.50; 6, 7 sample QE 15.00, Zone CNP7. 8-11 *Lithoptychius varoli.* 8, 10, 11 sample QE 8.30; 9 sample QE 8.60, Subzone CNP5b 12, 13 *Lithoptychius collaris.* 12 sample QE 11.40, 13 sample QE 8.30, Zone CNP7. 14-20 *Lithoptychius felis*. 14-17, 19, sample QE 8.30, 18 sample QE 8.60, CNP5b; 20 sample QE 9.22, Zone CNP6. 21- 25 *Lithoptychius schmitzii*. Sample 21, 23 sample QE 8.30, 22, 25 sample QE 10.30, 24 sample QE 11.10, Subzone CNP5b.

References

Abdel Hameed, A.T., and Faris, M., 1984. Changes of relative surface water temperature through the Maastrichtian-Ypresian in central Egypt. Middle East Research Centre, Ain Shams Univ., Earth Science, Feb 02, 1984.

Abdel Razik, T.M., 1972. Comparative studies on the Upper Cretaceous–Early Paleogene sediments on the Red Sea coast, Nile Valley and Western Desert, Egypt. 6th Arab Petroleum Congress, Algeria, 71, pp. 1–23.

Agnini, C., Muttoni, G., Kent, D.V., and Rio, D., 2006. Eocene biostratigraphy and magnetic stratigraphy from Possagno, Italy: the calcareous nannofossil response to climate variability, Earth. Planet. Sc. Lett., 241, pp. 815–830.

Agnini, C., Fornaciari, E., Raffi, I., Rio, D., Röhl, U., and Westerhold, T., 2007. High-resolution nannofossil biochronology

of middle Paleocene to early Eocene at ODP Site 1262: implications for calcareous nannoplankton evolution. Marine Micropaleontology, 64 (2007), pp. 215-248.

Agnini, C., Fornaciari, E., Raffi, I., Catanzariti, R., Pälike, H., Backman, J., and Rio, D., 2014. Biozonation and biochronology of Paleogene calcareous nannofossils from low and middle latitudes. Newsletters on stratigraphy, V. 47/2 (2014), pp. 131-181, Stuttgart.

Arney, J., and Wise, S.W., 2003. Paleocene-Eocene nannofossil biostratigraphy of ODP Leg 183, Kerguelen Plateau. In: Frey, FA; Coffin, MF; Wallace, PJ; Quilty, PG (eds.). Proceedings of the Ocean Drilling Program, Scientific Results, College Station, TX (Ocean Drilling Program), 183, pp. 1-59.

Aubry, M-P., and Salem, R., 2013a. The Dababiya Quarry Core: Coccolith Biostratigraphy. Stratigraphy, V. 9 (2012) (2013), pp. 241–259.

Aubry, M-P., and Salem, R., 2013b. The Dababiya Core: a window into Paleocene to Early Eocene depositional history in Egypt based on coccolith stratigraphy. Stratigraphy V. 9 (2012) (2013), pp. 287–346.

Aubry, M.-P., 1998. Early Paleogene calcareous nannoplankton evolution: a tale of climatic amelioration. In: Aubry, M.-P., Ouda, K. (Eds.), Late Paleocene–early Eocene Biotic and Climatic Events in the Marine and Terrestrial Record Columbia University Press, New York, pp. 158–201.

Aubry, M.-P., Rodriguez, O., Bord, D., Godfrey, L., Schmitz, B., and Knox, R., 2012. The First Radiation of the *Fasciculiths*: Morphologic adaptations of the coccolithophores to oligotrophy. Austrian Journal of Earth Sciences, 105, pp. 29–38.

Awad, G.H., and Ghobrial, M.G., 1965. Zonal Stratigraphy of the Kharga Oasis. Ministry of Industry, General Egyptian Organization for Geological Research and Mining, Geological Survey, Cairo, paper no. 34, pp. 1-77.

Barazi, N. and Kuss, J., 1987. Southernmost outcrops of marine Lower Tertiary carbonates rocks in NE-Africa (Gabal Abyad, Sudan), Geological Rundschau, Stuttgart (1987), 76, pp. 529-537.

Bassiouni, M.A., Faris, M., and Sharaby, S., 1991. Late Maastrichtian and Paleocene calcareous nannofossils from Ain Dabadib section, NW Kharga Oasis. Qatar University Science Bulletin, 11 (1991), pp. 357–375.

Bernaola, G., Baceta, J.I., Orue-Extebarria, X., Alegret, L., Martin-Rubio, M., Arostegui, J., and Dinarès-Turell, J., 2007. Evidence of an abrupt environmental disruption during the mid-Paleocene biotic event (Zumaia section, western Pyrenees). Geological Society of America Bulletin, 119 (2007), pp. 785–795.

Bernaola, G., Martín-Rubio, M., and Baceta, J.I., 2009. New high resolution calcareous nannofossil analysis across the Danian/Selandian transition at the Zumaia section: comparison with South Tethys and Danish sections. Geologica Acta, 7 (2009), pp. 79–92.

Bornemann, A., 2003. Case studies of Mesozoic calcareous nannofossils: Implications for paleoecology, calcareous nannofossil morphology and carbonate accumulation. PhD Thesis, Ruhr-University, Bochum, 2003, 126 pp.

Bornemann, A., Schulte, P., Sprong, J., Steurbaut, E., Youssef, M., and Speijer, R.P., 2009. Latest Danian carbon isotope anomaly and associated environmental change in the Southern Tethys (Nile Basin, Egypt). Journal of the Geological Society of London, 166 (2009), pp. 1135–1142.

Bown, P.R., and Pearson, P., 2009. Calcareous plankton evolution and the Paleocene/Eocene thermal maximum event: New evidence from Tanzania. Marine Micropaleontology 71, pp. 60-70.

Bralower, T.J., 2002. Evidence of surface water oligotrophy during the Paleocene-Eocene thermal maximum: Nannofossil assemblage data from Ocean Drilling Program Site 690, Maud Rise, Weddell Sea. Paleoceanography 17, pp.

Dinarès-Turell, J., Stoykova, K., Baceta, J.I., Ivanov, M., and Pujalte, V., 2010. High-resolution intra- and interbasinal correlation of the Danian–Selandian transition (Early Paleocene): the Bjala section (Bulgaria) and the Selandian GSSP at Zumaia (Spain). Paleogeography, Paleoclimatology and Paleoecology, 297 (2) (2010), pp. 511–533.

Eshet, Y., and Almogi Labin, A., 1996. Calcareous nannofossils as paleoproductivity indicators in Upper Cretaceous organic-rich sequences in Israel. Marine Micropaleontology, 29 (1996), pp. 37–61.

Faris, M., and Farouk, S., 2012. Integrated biostratigraphy of two Upper Maastrichtian-Paleocene successions in north-central Sinai, Egypt. Geologia Croatica, pp. 139-160, 65/2, Zagreb, 2012.

Fuqua, L., Bralower, T., Arthur, M., and Patzkowsky, M., 2008. Evolution of calcareous nannoplankton and recovery of marine food webs after the Cretaceous–Paleocene mass extinction. Palaios, 23 (2008), pp. 185–194.

Guasti, E., Speijer, R.P., Fornaciari, E., Schmitz, B., Kroon, D., and Gharaibeh, A., 2005. Transient biotic change within the Danian–Selandian transition in Egypt and Jordan. Chapter IV of PhD E. Guasti, Early Paleogene environmental turnover in the Southern Tethys as recorded by foraminiferal and organic-walled dinoflagellate cysts assemblages. Berichte aus dem Fachbereich Geowissenschaften der Universität Bremen, pp. 75–110.

Gibbs, S.J., Bown, P.R., and Bralower, T.J., 2006. Ocean acidification and calcareous nannoplankton at the Paleocene–Eocene Thermal Maximum. F. Caballero (Ed.) et al., Climate and Biota of the Early Paleogene (2006), pp. 51. Abstract, Bilbao.

Guasti, E., Speijer, R.P., Brinkhuis, H., Smit, J., and Steurbaut, E., 2006. Paleoenvironmental change at the Danian–Selandian transition in Tunisia; Foraminifera, organic-walled dinoflagellate cyst and calcareous nannofossil records. Marine Micropaleontology, 59 (2006), pp. 210–229.

Guiraud R., and Bosworth W., 1999. Phanerozoic geodynamic evolution of northeastern Africa and the northwestern Arabian platform. Tectonophysics, 315 (1999), pp. 73–108.

Hammer, Ø., Harper, D.A., and Ryan, P.D., 2001. Past: paleontological statistics software package for education and data analysis. Palaeontologia Electronica, 4(1), pp.1-9.

Haq, B.U., and Lohmann, G.P., 1976. Early Cenozoic calcareous nannoplankton biogeography of the Atlantic Ocean. Marine Micropaleontology, 1 (1976), pp. 119–194.

Haq, B.U., Lohmann G.P., and Wise S.W., 1976: Calcareous nannoplankton biogeography and its paleoclimatic implications: Cenozoic of Falkland Plateau (DSDP Leg 36) and Miocene of the Atlantic Ocean Initial Report Deep Sea Drilling Project, 36 (1976), pp. 745–760.

Kasem, A. M., 2016. Stratigraphical and Micropaleontological Studies on Some Upper Cretaceous–Lower Paleogene Successions in Egypt. PhD Thesis, Damanhour University, 2016, 214 pp.

Kasem A.M. (2023). Lithostratigraphy, Stable Isotope Stratigraphy and Calcareous Nannofossils Biostratigraphy of the Danian-Thanetian at Nukhul, Sinai, Egypt.

Frontiers in Scientific Research and Technology Journal, 5 (2023), pp. 73 – 83.

Kasem A.M. and Kassab W. G., 2023.Upper Paleocene–lower Eocene calcareous nannofossil biostratigraphy at Nukhul, West Central Sinai, Egypt. Journal of Umm Al-Qura University for Applied Sciences. https://doi.org/10.1007/s43994-023-00104-y.

Kasem A.M., Faris M., JovaneL., Ads T., A., Frontalini F., Zaky A., S., 2022. Biostratigraphy and Paleoenvironmental Reconstruction at the Gebel Nezzazat (Central Sinai, Egypt): A Paleocene Record for the Southern Tethys. Geosciences 2022, 12, 96,1-22. https://doi.org/10.3390/geosciences12020096

Kasem, A., M., Wise, Jr., Faris, M., Farouk, S., Zahran, E., 2017. Calcareous nannofossil biostratigraphy of the Paleocene at the Misheiti section, East Central Sinai, Egypt. Arabian Journal of Geosciences (2017): 10-455. DOI 10.1007/s12517-017-3217-4.

Knox, R.W.O'B., Aubry, M-P., Berggren, W.A., Dupuis, C., Ouda, K., Magioncalda, R., and Soliman, M., 2003. The Qreiya section at Gebel Abu Had: lithostratigraphy, clay mineralogy, geochemistry and biostratigraphy. Micropaleontology, 49 (2003), pp. 93–104.

Martini, E., 1971. Standard Tertiary and Quaternary calcareous nannoplankton zonation. In: Farinacci, A. (Eds.), Proceedings of the II Planktonic Conference 2, Roma (1970), pp. 739-785.

Monechi, S., Reale, V., Bernaola, G., and Balestra, B., 2013. The Danian/Selandian boundary at Site 1262 (South Atlantic) and in the Tethyan region: biomagnetostratigraphy, evolutionary trends in fasciculiths and environmental effects of the Latest Danian Event. Marine Micropaleontology, 98 (2013), pp. 28–40.

Mutterlose, J., Linnert, C., and Norris, R., 2007. Calcareous nannofossils from the Paleocene–Eocene thermal maximum of the equatorial Atlantic (ODP Site 1260B): evidence for tropical warming. Marine Micropaleontology, 65 (2007), pp. 13–31.

Obaidalla, N.A., El-Dawy, M.H., and Kassad, A.S., 2009. Biostratigraphy and paleoenvironment of the Danian/Selandian (D/S) transition in the Southern Tethys: a case study from north Eastern Desert, Egypt. Journal of African Earth Sciences, 53 (2009), pp. 1–15.

Omara, S., Philobbos, E.R., and Mansour, H.H., 1976. Contribution to the Lithostratigraphy and epeirogenesis of the Dakhla Oasis area, Western Desert, Egypt. Bull. FBC. Sci. Assiut Univ., 5(3), pp. 319-340.

Pospichal, J., and Wise, S.W. Jr., 1990. Paleocene to middle Eocene calcareous nannofossils of ODP Sites 689 and 690, Maud Rise, Weddell Sea ,in: P.R. Barker, J.P. Kennett (Eds.) et al., ODP, Sci. Results, v. 113Ocean Drilling Program, College Station, TX (1990), pp. 613–638.

Quillévéré, F., Aubry, M.-P., Norris, R.D., and Berggren, W.A., 2002. Paleocene oceanography of the eastern subtropical Indian Ocean: an integrated magnetobiostratigraphic and stable isotope study of ODP Hole 761B (Wombat Plateau). Paleogeography, Paleoclimatology and Paleoecology, 184 (3–4) (2002), pp. 371–405.

Quillévéré, F., Norris, R.D., Kroon, D., and Wilson, P.A., 2008. Transient Ocean warming and shifts in carbon reservoirs during the early Danian. Earth and Planetary Science Letters, 265 (2008), pp. 600–615

Rodríguea, O., and Aubry, M.-P., 2006. Lower to Middle (Danian–Selandian) Paleocene calcareous nannofossil stratigraphy of the Qreiya Section (Egypt). In: Sixth International Conference on the Climate and Biota of the Early Paleogene. Abstract, pp. 111.

Said, R., 1961. Tectonic framework of Egypt and its influence on distribution of foraminifera. Am. Assoc. Petroleum Geologists Bull., 45 (1961), p. 198–218.

Said, R., 1962. The Geology of Egypt. Elsevier, Amsterdam (1962), pp. 1–377.

Schmitz B., Pujalte V., Molina E., Monechi S., Orue-Etxebarria X., Speijer R.P., Alegret L., Apellaniz E., Arenillas I., Aubry M.-P., Baceta J.-I., Berggren W.A., Bernaola G., Caballero F., Clemmensen A., Dinarès-Turell J., Dupuis C., Heilmann-Clausen C., Orús A.H., Knox R., Martín-Rubio M., Ortiz S., Payros A., Petrizzo M.-R., Von Salis K., Sprong J., Steurbaut E., and Thomsen E., 2011. The Global Stratotype Sections and Points for the bases of the Selandian (Middle Paleocene) and Thanetian (Upper Paleocene) stages at Zumaia, Spain. Episodes, 34 (2011), pp. 220–243.

Soliman, M.F., and Obaidalla, N.A., 2010. Danian–Selandian transition at the Gabal el-Qreiya section, Nile Valley (Egypt): lithostratigraphy, biostratigraphy, mineralogy and geochemistry. Neues Jahrbuch für Geologie und Paläontologie, 258 (2010), pp. 1–30.

Speijer, R.P., 2003a. Systematics and paleoecology of the foraminifer Neoeponides duwi (Nakkady) from the Paleocene of Egypt. Micropaleontology, 49 (2003), pp. 146–150.

Speijer, R.P., 2003b. Danian–Selandian sea-level change and biotic excursion on the southern Tethyan margin, in: S.L. Wing, P.D. Gingerich, B. Schmitz, E. Thomas (Eds.), Causes and consequences of globally warm climates in the Early Paleogene, Geological Society of America Special Paper 369 (2003), pp. 275–290.

Sprong, J., Speijer, R.P., and Steurbaut, E., 2009. Biostratigraphy of the Danian/Selandian transition in the southern Tethys. Special reference to the lowest occurrence of planktic foraminifera Igorina albeari. Geologica Acta, 7 (2009), pp. 63–77.

Sprong, J., Youssef, M., Bornemann, A., Schulte, P., Stassen, P., Steurbaut, E., Kouwenhovens, T.J., and Speijer, R.P., 2011. A multi-proxy record of the Latest Danian Event at Gebel Qreiya, Eastern Desert, Egypt. Journal of Micropalaeontology, 30 (2011), pp. 167–182.

Sprong, J., Kouwenhovens, T.J., Bornemann, A., Dupuis, C., Speijer, R.P., Stassen, P., and Steurbaut, E., 2013. In search of the Latest Danian Event in a paleobathymetric transect off Kasserine Island, north-central Tunisia. Paleogeography, Paleoclimatology and Paleoecology, V. 379-380 (2013), pp. 1-16.

Steurbaut, E., and Sztrákos, K., 2008. Danian/Selandian boundary criteria and North Sea basin–Tethys correlation based on calcareous nannofossil and foraminiferal trends in SW France. Marine Micropaleontology, 67 (2008), pp. 1–29.

Steurbaut, E., Dupuis, C., Arenillas, I., Molina, E., and Matmati, M.F., 2000. The Kalaat Senan section in central Tunisia: a potential reference section for the Danian/Selandian boundary GFF, 122 (2000), pp. 158–160.

Thibault, N., and Gardin, S., 2007. The late Maastrichtian nannofossil record of climate change in the South Atlantic DSDP Hole 525A. Marine Micropaleontology 65, pp. 163–184.

Tremolada, F., Erba, E., and Bralower, T.J., 2007. A review of calcareous nannofossil changes during the early Aptian oceanic anoxic event 1a and the Paleocene–Eocene thermal maximum: the influence of fertility, temperature, and pCO2,in: S. Monechi, R. Coccioni, M.R. Rampino (Eds.), Large Ecosystem Perturbations: Causes and Consequences, Geological Society of America, Special Paper 424 (2007), pp. 87–96.

Varol, O., 1989. Palaeocene calcareous nannofossil biostratigraphy. In: J.A. Crux, S.E. Van Heck (Eds.), Nannofossils and Their Applications, British Micropaleontological Society. Ser, 12 (1989), pp. 267–310.

Wei, W., and Wise, S.W.Jr., 1990. Biogeographic gradients of middle Eocene-Oligocene calcareous nannoplankton in the South Atlantic Ocean. Palaeogeography Palaeoclimatology Palaeoecology 79, pp. 29–61.

Westerhold, T., Röhl, U., Raffi, I., Fornaciari, E., Monechi, S., Reale, V., Bowles, J., and Evans, H.F., 2008. Astronomical calibration of the Paleocene Time. Palaeogeography, Palaeoclimatology, Palaeoecology, 257 (2008), pp. 377–403.

Westerhold, T., Röhl, U., Donner, B., McCarren, H.K., and Zachos, J., 2011. A complete high-resolution Paleocene benthic stable isotope record for the central Pacific (ODP Site 1209). Paleoceanography, 26 (2011), p. PA2216.

Winter, A., Jordan, R.W., and Roth, P.H., l994. Biogeography of living coccolithophores in ocean waters. In: Winter, A., Siesser, W.G. (Eds.), Coccolithophores. Cambridge Univ. Press, Cambridge, pp. l6l-l78.

Wise S.W.Jr., and Wind, F.H., 1977. Mesozoic and Cenozoic calcareous nannofossils recovered by DSDP Leg 36 drilling on the Falkland Plateau, southwest Atlantic sector of the Southern Ocean. Proceeding of Deep Sea Project Initial Reports, 36 (1977), pp. 269–491.

Youssef, M., 2009. High resolution calcareous nannofossil biostratigraphy and paleoecology across the Latest Danian Event (LDE) in central Eastern Desert, Egypt. Marine Micropaleontology, 72 (2009), pp. 111–128.